IET Renewable Power Generation

Research Article

IET Journals
The Institution of Engineering and Technology

Highly sensitive microgrid protection using overcurrent relays with a novel relay characteristic

ISSN 1752-1416
Received on 5th July 2019
Revised 25th November 2019
Accepted on 23rd January 2020
E-First on 3rd March 2020
doi: 10.1049/iet-rpg.2019.0793
www.ietdl.org

Ahmad Darabi[1] ✉, Mehdi Bagheri[1], Gevork B. Gharehpetian[2]

[1]*Electrical Engineering Department, Nazarbayev University, Nur-Sultan, Kazakhstan*
[2]*Electrical Engineering Department, Amirkabir University of Technology, Tehran, Iran*
✉ *E-mail: ahmad.darabi@nu.edu.kz*

Abstract: Following the high penetration of synchronous generators (SGs) in the power network, optimal overcurrent coordination improvement under faulty conditions has become a crucial problem. To reduce the overcurrent relay operating time, a new overcurrent relay curve is proposed in this study. Then, the overcurrent coordination problem is overcome by using a robust combinatorial optimisation method. Additionally, SG sizing and location is performed to verify the merits of both the proposed relay curve and the applied optimisation algorithm. The proposed relay curve performance is compared with other non-standard relays characteristic available in the literature for a standard microgrid. Then, the proposed relay curve is applied to both the 8-bus transmission and the 33 kV distribution portion of the 30-bus IEEE standard power test systems. Then, the SG transient stability for different fault locations is analysed. Finally, an accurate comparison between the proposed relay curve and standard/non-standard curves available in the literature is provided by applying the same optimisation method and network topology. The simulation results confirm the superiority of the proposed relay curve.

1 Introduction

The dispersed contribution of distributed generation benefits the power network from several aspects [1–3]. The presence of distributed generation has led to a huge evolution in the power system configuration from past radial topologies to modern meshed networks. Hence, variations in the magnitude and direction of fault currents are overt consequences of power network reconfigurations [2, 4–6]. Protective devices are the most important items that address these changes. A directional overcurrent relay (DOCR) is the most common protective device because of its economic [7–9] and easy implementation compared with fuses and reclosers [10–12]. DOCRs act as the primary protection in distribution networks and the secondary protection in transmission networks [4, 7–9, 13, 14]. The sensitivity, selectivity and reliability are determinant factors in overcurrent coordination [4, 7, 9, 12, 15, 16]. In case of any electrical fault in the power network, the relay with the shortest electrical distance to the fault point should react first, and then, its backup protection should trip after a specific time, known as the coordination time interval, elapses. This quantity is typically chosen to be between 0.2 and 0.5 s in the literature and is set to 0.3 s in this paper. Encouraging proposals to accomplish overcurrent coordination have been published in the literature such as adaptive protection [3, 4, 17–22], fault current limiter installation to mitigate the impact of distributed generation [1, 23–27], restriction of distributed generation in faulty conditions [28], fault ride-through control of the inverter [2, 29–31], optimal distributed generator (DG) location and sizing [1, 32], planning schemes [24, 25], clustering [33] and communication-based dual setting methods [15, 16, 34]. Some demerits of each scheme are outlined in [3]. Minimising relay operating times while considering coordination constraints is a non-linear programming optimisation problem. To solve this problem, various metaheuristic algorithms [3, 13, 27, 32, 35–38] deterministic algorithms [7, 14, 15, 24, 39] and their combination [22, 26, 40–43] have been employed in the literature. In our previous study [43], the merits and demerits of each optimisation approach were discussed in detail. Afterwards, a novel combinatorial optimisation method was proposed in [43] such that each approach's advantages overlap the disadvantages of the other approaches. As a notable result, the obtained results for noncommunication-based overcurrent coordination were in the range of communication-based dual setting schemes. Hence, the applied optimisation algorithm in [43] is improved in this paper through the following changes. The metaheuristic part in [43] comprises the parallel execution of a genetic algorithm (GA) and particle swarm optimisation (PSO). To reduce the algorithm complexity and operating time, the GA–PSO configuration is superseded by a differential evolutionary (DE) algorithm in this paper. In other words, Rosen's gradient projection (RGP) [44] is executed in series with DE. The RGP–DE loop is iterated until the results converge. Then, Zoutendijk's method [44] is implemented. Although the relay operating time can be significantly reduced using a prominent optimisation method, this reduction is restricted due to relay characteristics. Consequently, different non-standard relay curves have occasionally been proposed in the literatures [45–49]. Some determinant factors should be taken into account to realise appropriate DOCR coordination utilising non-standard curves.

First, deterministic methods are inherently incapable of removing miscoordinations. Hence, the metaheuristic algorithms are responsible for violation elimination. However, highly incongruous characteristics of relay curves impede the metaheuristic part from removing violations in some cases, and consequently, a catalyser is needed. As an appropriate catalyser, an objective function (OF) similar to the fitness function proposed in our previous work [43] is used for this paper in Section 2, and the miscoordination elimination method described in [43] is implemented in this paper. To obtain a more reliable coordination, miscoordinations for both near- and far-end faults are taken into account in the OF.

Additionally, violations are treated with a large penalty in the applied fitness function. Second, though the electrical fault distance to the relay location is often commensurate with the voltage of the relay position, this premise is not generic for all cases. Hence, the curve dependency on the voltage drop (for non-standard curves that are dependent on the voltage drop) should be carefully controlled by the other parameters. This fact is discussed in detail in Section 3. Third, the non-standard relay curve should be chosen to prevent discrimination times from reaching unfavourably large values. If discrimination times become very large, then fault damages can more rapidly disseminate to far electrical distances. This case is studied in detail in Section 4. Fourth, selecting new

Table 1 IEC standard relays [50]

Relay type	*A*	*B*	*C*
SI	0.14	0.02	0
VI	13.5	1	0
EI	80	2	0

curve characteristics is usually equivalent to introducing new optimisation variables [45–49]. Existing optimisation techniques should overcome several challenges to find the global optima for time setting multipliers (TSMs) and plug setting multipliers (PSMs). An increasing number of design variables makes the situation more critical. The design variable numbers for the relay curves proposed in [45–47] are 6, 3, and 4, respectively. This quantity is three for the proposed relay curve considering the previous challenges. The relay curve proposed in [48] gives a zero second operating time for electrical faults occurring in front of the relay (i.e. zero electrical distance), and consequently, transient faults are neglected in the relay performance. A complete review of the proposed non-standard relays can be found in [49] and is not discussed here for brevity.

In the next section, all coordination constraints and formulations are given. Then, the proposed relay curve is presented in Section 3. In Section 4, the obtained results are provided, and the final section is devoted to the conclusion.

2 Problem formulation

2.1 Relay curves

The International Electrotechnical Commission (IEC) standard relay curve formulation is given by [50]

$$t_{\text{op}} = \frac{A \times \text{TSM}}{(I_{\text{f}}/I_{pickup})^{B} - 1} + C, \tag{1}$$

and the non-standard relay proposed by Saleh *et al.* [46] is as follows:

$$t_{\text{op}} = \text{e}^{(V_{\text{f}}-1).K} \frac{A \times \text{TSM}}{(I_{\text{f}}/I_{pickup})^{B} - 1}, \tag{2}$$

where I_{f}, I_{pickup}, V_{f}, and K are the fault current measured by the relay, relay pickup current (PSM.I_{loadmax}), the voltage at the relay location, and a new optimisation variable, respectively. Overcurrent relays can be categorised into three groups: standard inverse (SI), very inverse (VI), and extremely inverse (EI). Coefficients A, B, and C are provided in Table 1 based on this categorisation.

2.2 OF and constraints

The applied fitness functions are given by (see (3))

$$\text{OF}_1 = \sum_{i=1}^{\text{RN}} (t_{i\text{mn}})^2 + \sum_{i=1}^{\text{RN}} (\Delta t_{i\text{n}})^2 \tag{4}$$

$$\Delta t_i = t_{i\text{b}} - t_{i\text{m}} - \text{CTI} \tag{5}$$

where *n, f*, *m*, *b*, MN, PN, and RN denote near end, far end, main relay, backup relay, the miscoordination number taking into account both near- and far-end faults, the total pair number, and the total relay number, respectively. Additionally, k_1 and k_2 have large values, and the *i*th pair discrimination time is defined by (5). The metaheuristic and deterministic parts utilise OF and OF_1, respectively. These selections are based on the properties of the metaheuristic and deterministic approaches [43]. According to the first note in Section 1, the removal of violations is accomplished via the metaheuristic part, and the OF utilised in (3) expedites this process. Consequently, reducing the relay operating and pair discrimination times is the secondary purposes of OF. In fact, searching over the entire design space to find a global optimum vicinity is the function of the metaheuristic part and OF. Therefore, the exploitation property of the optimiser is augmented using DE and OF. In contrast, the miscoordination elimination term is neglected in OF_1, considering that constraint violations are avoided because of the inherent characteristic of deterministic methods. Hence, minimising both the relay discrimination and pair discrimination times is the distinct objective of both the deterministic part and OF_1. As a notable consequence, the exploitation property of the optimiser is augmented using a prominent deterministic approach and OF_1. The relay operating time (for near-end faults) may significantly decrease when using DOCRs with non-standard curves. This increase in relay sensitivity may lead to sympathetic trips for transient faults. This phenomenon is seldom observed when DOCRs with standard curves are used for coordination because the operating time of standard curves is usually sufficiently high. Consequently, this issue should be taken into account in the optimisation constraints. On the basis of the above discussion, the minimum relay operating times should be taken into account in the constraints, and finally, the entire coordination constraints can be considered as (6)–(10). The optimiser and fitness function proposed in [43] have led to prominent results for DOCR coordination using only SI curves in the range of dual setting schemes

$$\Delta t_{\text{in}} \geq 0 \tag{6}$$

for $i = 1{:}\text{PN}$

$$\Delta t_{\text{if}} \geq 0 \tag{7}$$

for $i = 1{:}\text{PN}$

$$1.2 \leq \text{PSM} \leq 1.6 \tag{8}$$

for $i = 1{:}\text{RN}$

$$\text{TSM}_{\text{min}} \leq \text{TSM}_i \leq \text{TSM}_{\text{max}} \tag{9}$$

for $i = 1{:}\text{RN}$

$$t_{\text{min}} \geq 0.05 \tag{10}$$

for $i = 1{:}\text{RN}$

3 Proposed relay curve

3.1 New non-standard relay curve

In DOCR coordination using the well known standard relay curves given by (1), optimal values for TSMs and PSMs (abiding by the coordination constraints) are explored in their corresponding design spaces. Then, DOCRs programmed with the standard relay curves (1) react following different possible faults depend only on the fault current measured by the relay, considering constant values for the previously obtained TSMs and PSMs. However, the voltage at the relay location can be taken into account in the relay curve equation to reduce the operating time [45–49]. Moreover, DOCRs have installed voltage sensors to discern the fault current direction.

$$\begin{aligned}\text{OF} = k_1 \cdot \text{MN} + \sum_{i=1}^{PN} (t_{i\text{mn}}^2 + t_{i\text{bf}}^2) + \sum_{i=1}^{\text{PN}} \{k_2(|\Delta t_{i\text{n}} - |\Delta t_{i\text{n}}|| + |\Delta t_{i\text{f}} - |\Delta t_{i\text{f}}||) \\ + (\Delta t_{i\text{n}} + |\Delta t_{i\text{n}}|)t_{i\text{bn}}^2 + (\Delta t_{i\text{f}} + |\Delta t_{i\text{f}}|)t_{i\text{bf}}^2\}\end{aligned} \tag{3}$$

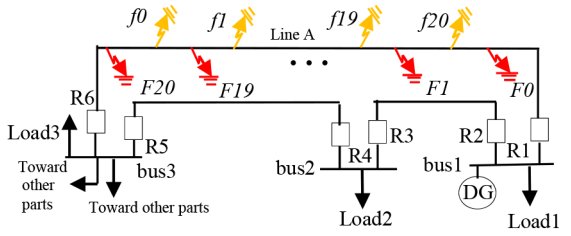

Fig. 1 *IEEE standard microgrid took from the 39-bus system*

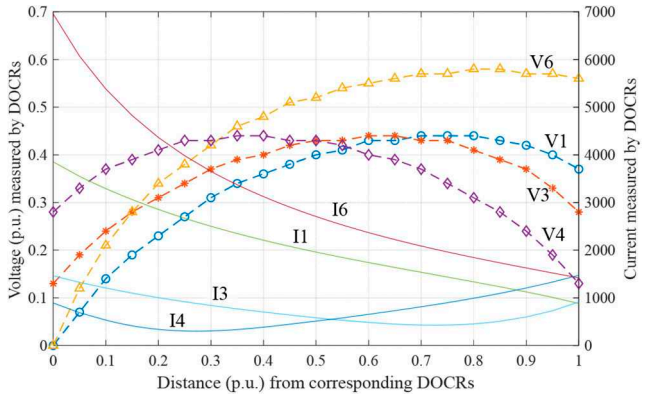

Fig. 2 *Currents and voltages sensed by R1–R3 and R6–R4 for faults on line A*

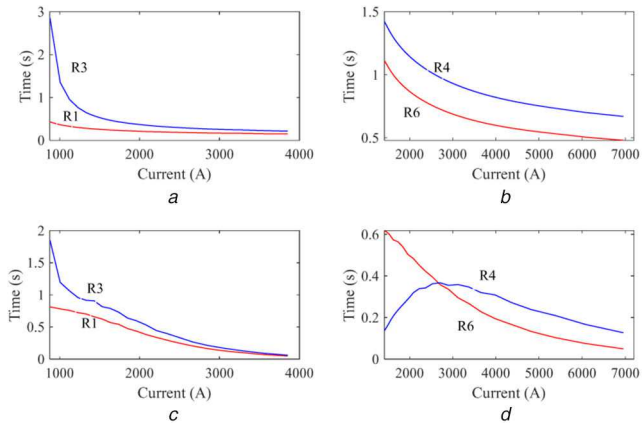

Fig. 3 *Performance of SI and non-standard curve in [46] for R1–R3 and R6–R4*

(a) R1–R3 reaction utilising SI curve (Table 1), ***(b)*** R6–R4 reaction utilising SI curve (Table 1), ***(c)*** R1–R3 reaction utilising curve proposed in [47], ***(d)*** R6–R4 reaction utilising curve proposed in [47]

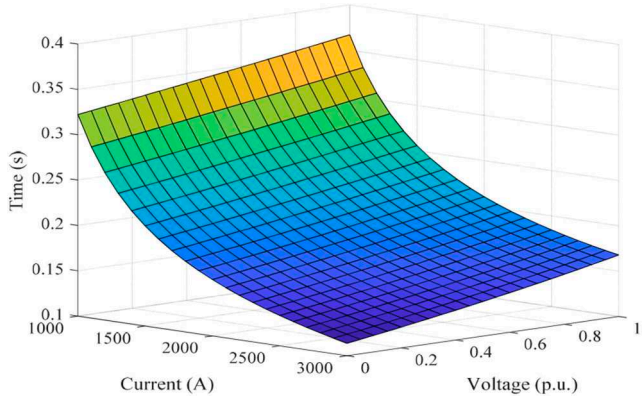

Fig. 4 *Performance of (11) under unusual fault voltage/current changes*

Additionally, a wide variety of non-standard relay curves can be adopted by microprocessor-based relays. The concept of involving the busbar voltage in the relay curve stems from the fact that the fault distance from a specific relay is proportional to the relay location voltage. However, this premise is valid for radial power systems, and in meshed power systems, the voltage magnitude at the relay location may decrease as the fault distance from the primary relay increases. This phenomenon depends on the network configuration and changes in the direction of the fault current flowing through DOCRs. The existence of multiple routes to feed a fault has made the meshed power systems susceptible to this issue. On the basis of the aforementioned discussion, the proposed non-standard relay curve in this paper is as follows:

$$t_{\text{op}} = \text{e}^{(I_{\text{f}}/I_{\text{f}}maxrelay)(V_{\text{f}}-1).K} \frac{A \times \text{TSM}}{(I_{\text{f}}/I_{pickup})^{B} - 1} \tag{11}$$

where $I_{\text{fmaxrelay}}$ and V_{f} are the maximum fault current that can flow from the DOCR (in front of the relay) and the voltage at the DOCR location. Additionally, coefficients A and B are the same as for the SI relays shown in Table 1, and the applied fitness functions and coordination constraints are given by (3)–(10).

3.2 Validation for a standard microgrid

To illustrate the problem mentioned in the previous section and Section 2, a small portion of the IEEE standard 39-bus transmission system is taken as a standard microgrid (Fig. 1). Then, possible faults on line A are emulated, and notable observations are provided. Faults F_0, F_1, F_2, …, F_{20} are simulated on 0, 5, 10, …, 100% of line A from R_1, respectively. Additionally, faults f_0, f_1, f_2, …, f_{20} are simulated on 0, 5, 10, …, 100% of line A from R_6, respectively. The measured voltages and currents of pairs R_1–R_3 and R_6–R_4 for the simulated faults on line A are depicted in Fig. 2.

On the basis of Fig. 2, all relay voltages begin to decrease when the fault distance from the primary relay exceeds a specific value. Hence, the antithesis to radial networks, the relay voltage may decrease as the fault point distance from the relay location increases in meshed power systems. Thus, ignoring this fact may eventually lead to curve distortion or even miscoordination in some cases.

The meshed configuration may lead to another phenomenon regarding current directions. Fig. 2 shows that the directions of I_3 and I_4 vary as the fault distance from R_1 and R_6 exceeds 73 and 28% of line A, respectively. Therefore, these incongruous variations in the sensed voltages and currents and their impacts on relay operating times should be taken into account in relay curves. To verify the above discussion numerically, the relay performance for simulated faults on line A using both the SI relay (Table 1) and the proposed non-standard relay in [46] are depicted in Fig. 3. In this figure, neither curve distortion nor pair miscoordination can be observed when SI relays (Table 1) are employed, despite the indicated unforeseen changes in voltages and currents. Additionally, the utilisation of DOCR voltages for the R_1–R_3 and R_6–R_4 pairs leads to significant decrements in their operating times. However, inappropriate distortions can be observed in the R_1–R_3 curves (Fig. 3*c*), and even worst, these distortions engender destructive protection failure in R_6–R_4. R_6–R_4 coordination can be preserved by moving the R_4 curve up in Fig. 3*d*; however, this approach leads to increased discrimination time for the corresponding pair. Moreover, curve distortion maybe more critical for other pairs.

On the basis of the problems above, a prominent relay curve capable of coping with the mentioned anomalies in voltage magnitudes and current directions is critically needed.

Next, to examine the performance of the relay curve proposed in this paper, the operating time obtained using (11) versus the measured current and voltage is depicted for R_1 in Fig. 4.

In the next step, the performance of the proposed relay curve in meshed microgrid configurations is examined.

Fig. 5 depicts the R_1–R_3 and R_6–R_4 operating times versus the currents and voltages measured by these relays. A notable fact that can be interpreted from Fig. 5*b* is that unforeseen changes in the voltages and currents measured by DOCRs are significantly damped. A comparison of Fig. 5*b* with Fig. 3*d* reveals this

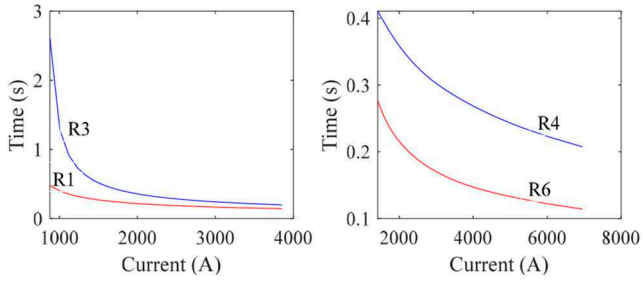

Fig. 5 *Performance of the proposed relay curves for R1–R3 and R6–R4*
(a) R1–R3 reaction utilising the proposed curve, ***(b)*** R6–R4 reaction utilising the proposed curve

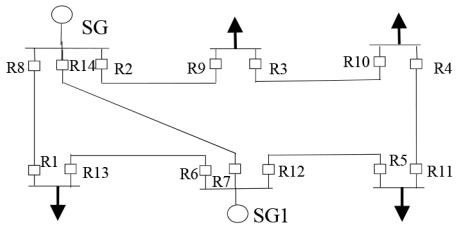

Fig. 6 *IEEE standard 8-bus power system*

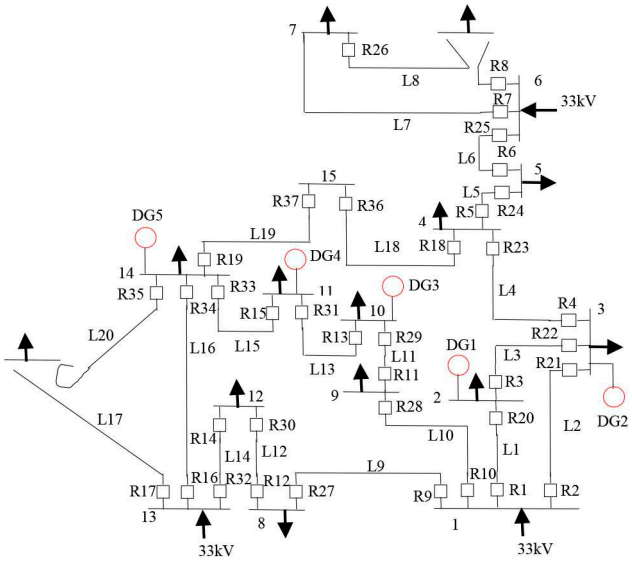

Fig. 7 *33 kV section of the IEEE standard 30-bus power system*

remarkable conclusion. Additionally, a comparison of Fig. 5*b* with Fig. 3*b* reveals no distortion in Fig. 5*b*. Unlike Fig. 3*c*, no distortion can be observed in Fig. 5*a*, and this fact can also be realised by juxtaposing Fig. 3*a* and 5*a*.

As the final validation of the proposed relay curve, the results obtained using the proposed relay curve are compared with the results obtained utilising the non-standard curve proposed in [46] considering the same optimiser and the same network topology in the following section.

4 Simulations and results

In this section, overcurrent coordination is achieved for both the 8-bus transmission (Fig. 6 and [51]) and the 33 kV portion of the 30-bus distribution (Fig. 7 and [52]) IEEE standard power test systems using the proposed relay curve. Afterwards, accurate comparisons between the values obtained with the proposed non-standard curve and other standard/non-standard curves available in the literature are provided. This section is divided into three sections. In the first section, the 8-bus transmission standard power system is taken for DOCR coordination, and the superiority of the proposed non-standard curve is verified by comparing the obtained results with those of the other methods. In the second section, the 33 kV portion of the 30-bus distribution IEEE standard power system is chosen for DOCR coordination. Additionally, five DGs are optimally located and sized according to coordination constraints and objectives. In the third section, DOCR coordination is accomplished using the non-standard relay curve proposed in [46] for the 30-bus distribution IEEE standard power system, and the network topology is assumed to be similar to that in the previous section.

As a prominent optimiser, the structure proposed in our previous work [43] is improved for this paper. On the basis of the deficiencies of the complex method discussed in [43], this method is eliminated from the optimiser. Additionally, to reduce the algorithm complexity, GA–PSO is replaced with DE, and the series combination of DE–RGP is executed until this combination converges. Then, the optimal values of TSM*s* are calculated using Zoutendijk's method. Although Zoutendijk's method is an Non-Linear Programming (NLP) solver, implementing this method to optimise all variables makes the entire algorithm sluggish.

4.1 DOCR coordination for the 8-bus system

The 8-bus IEEE standard transmission power system is depicted in Fig. 6, and the corresponding data on this network are given in [51]. Overcurrent coordination using both the non-standard curve proposed in this paper and the non-standard curve proposed in [46] has been performed considering the same optimiser (DE–RGP–Zoutendijk method) and the same network data. Hence, an accurate comparison can be expected by applying the same coordination and network conditions. The optimised values obtained from both (2) and (11) are provided in Tables 2 and 3, respectively. In these tables, RN, PN, DT, and (*m, b*) denote the relay number, pair number, discrimination time, and (main, backup) coordination pair, respectively.

A comparison of the total operating times shown in Tables 2 and 4 reveals a reduction of 64.7% in the total operating time for overcurrent coordination when using (11), taking into account the same conditions. Additionally, a simple comparison shows that the average discrimination times for both cases are roughly equal. For further evaluation, the results given in Tables 2 and 3 are compared with the values obtained from other optimisers and IEC standard relays for the same power system in Table 4. As per Table 4, the value of 2.27 s for the summation of relay operating times confirms the significant improvement in DOCR coordination when using the proposed non-standard relay.

As previously mentioned in Section 1, distance and overcurrent relaying are the primary and secondary protections in transmission power networks, respectively. Accordingly, overcurrent coordination has been performed for the 8-bus power transmission network to provide a comparison between the proposed method and other schemes available in the literature.

Table 4 shows that once the red, green, and blue implemented in the optimiser structure, the total relays operating time has significantly reduced in many cases. In [43], an optimiser including GA, PSO, RGP, and complex method has been proposed. The recent combination has notably reduced the total relays operating time (6.907 s) as compared with other optimisers such as conventional GA (11 s), hybrid GA– Linear Programming (LP) (10.95 s), GA–PSO (10.67 s), fuzzy-GA (9.636 s), and the seeker algorithm (8.427 s). Particularly, the total relays operating time dropped to 2.2741 s using the proposed method and satisfying coordination constraints. The obtained results using the proposed approach are in the range of 1/5th of the results achieved using the conventional methods (Table 4).

4.2 DOCR coordination for the 30-bus system

In the following, optimal TSM, PSM, and *K* values and optimal synchronous generator (SG) sizes and locations for the 30-bus standard distribution system (Fig. 7) are obtained. SGs considerably contribute to fault currents compared with inverter-based DGs. Moreover, the contribution of inverter-based DGs to fault currents can be significantly controlled [2, 29–31]. Therefore, only synchronous-based DGs are considered in DOCR coordination.

Table 2 DOCR coordination obtained using the curve proposed in [46]

RN	TSM	PSM	K	$T_{operation}$	PN	(m,b)	DT
1	1.5084	1.5177	1.6093	0.6227s	1	(2,1)	0.5046
2	2.1311	1.2868	3.0439	0.2951	2	(14,1)	0.3763
3	2.1163	1.5899	2.3759	0.5108	3	(3,2)	0.0000
4	1.0307	1.4413	1.5314	0.5679	4	(4,3)	0.0000
5	0.3366	1.2047	1.5520	0.3602	5	(5,4)	0.1786
6	2.5985	1.4176	2.2302	0.5112	6	(6,5)	0.0000
7	3.6013	1.4582	2.7359	0.4138	7	(7,5)	0.0974
8	4.0000	1.6000	2.5637	0.5370	8	(1,6)	0.0487
9	3.9682	1.2384	3.9225	0.3558	9	(2,7)	0.2419
10	2.2550	1.4106	2.2869	0.5501	10	(8,7)	0.0000
11	4.0000	1.6000	3.2187	0.4283	11	(13,8)	0.1927
12	2.0393	1.5764	3.3334	0.2499	12	(8,9)	0.1022
13	2.5089	1.3205	2.2094	0.6144	13	(14,9)	0.2157
14	3.8440	1.3842	2.7653	0.4234	14	(9,10)	0.2478
					15	(10,11)	0.0000
					16	(11,12)	0.0000
					17	(7,13)	0.4021
					18	(12,13)	0.5659
					19	(6,14)	0.0000
					20	(12,14)	0.2613
sum $T_{operation}$	6.4406 s		average DT = 0.1718 s				

Table 3 DOCR coordination obtained using the proposed curve

RN	TSM	PSM	K	$T_{operation}$	PN	(m,b)	DT
1	0.6225	1.2919	2.9997	0.0609	1	(2,1)	0.2711
2	0.2016	1.3848	0.9913	0.2246	2	(14,1)	0.4457
3	0.4166	1.2663	1.5943	0.2017	3	(3,2)	0.0000
4	0.2757	1.4838	1.2628	0.2010	4	(4,3)	0.0000
5	0.1068	1.3573	2.2453	0.0627	5	(5,4)	0.0665
6	0.4261	1.5747	2.3687	0.0752	6	(6,5)	0.0956
7	0.5170	1.4517	2.4960	0.0754	7	(7,5)	0.0954
8	0.4329	1.5015	0.9739	0.2802	8	(1,6)	0.0000
9	0.0882	1.5056	0.3455	0.3252	9	(2,7)	0.0556
10	1.2069	1.2229	3.0000	0.1372	10	(8,7)	0.0000
11	0.2744	1.3682	0.7197	0.3364	11	(13,8)	0.2170
12	0.5010	1.3576	2.4499	0.1380	12	(8,9)	0.3478
13	0.5029	1.4075	2.3844	0.1057	13	(14,9)	0.5779
14	0.5754	1.3722	2.9999	0.0500	14	(9,10)	0.0000
					15	(10,11)	0.1304
					16	(11,12)	0.0000
					17	(7,13)	0.5060
					18	(12,13)	0.4434
					19	(6,14)	0.1575
					20	(12,14)	0.0947
sum $T_{operation}$	2.2741 s		average DT = 0.1752 s				

Table 4 DOCR coordination using various optimisers and curves

Method	Relay curve	$\sum t_{op\text{-}primary}$, s
fuzzy-GA [9]	SI	9.636
GA–PSO [43]	SI	10.67
GA–PSO–RGP complex [43]	SI	6.907
seeker [13]	SI	8.427
conventional GA [40]	SI	11
hybrid GA–LP [40]	SI	10.95
GA–PSO–RGP complex [43]	SI, VI, EI	4.4088
DE–RGP–Zoutendijk (Table 2)	non-standard [46]	6.4406
DE–RGP–Zoutendijk (Table 3)	proposed non-standard (10)	2.2741

Table 5 Optimum DG location and size

DG number	Size	Location
1	P = 4.8 MW, Q = 2.5 MVar	bus 2
2	P = 4.6 MW, Q = 2.9 MVar	bus 3
3	P = 3.2 MW, Q = 1.1 MVar	bus 10
4	P = 4.2 MW, Q = 1.8 MVar	bus 11
5	P = 3.3 MW, Q = 3.9 MVar	bus 14

Then, the algorithm implemented to calculate the relay load and fault currents is demonstrated. First, the $\boldsymbol{Y}_{\text{bus}}$ matrix of the initial power system without any DG installation is calculated before entering the optimisation loop. Each DG is modelled by a series combination of its internal impedance and excitation voltage. Then, the value of the DG excitation voltage is calculated considering the obtained DG capacity and location (using the DE algorithm) and considering 1 pu as the prefault voltage of DG busbars. Afterwards, busbar voltages for the normal operation mode are obtained using the Kirchhoff's current law and the obtained $\boldsymbol{Y}_{\text{bus}}$ (in the first step) and excitation voltages (in the second step).

Consequently, the relay currents are calculated in the next step. A similar process is implemented to determine the DOCR currents and voltages in faulty conditions. The only difference is that Y_{busf} describing a fault occurrence at bus j is calculated by omitting the jth row and column from $\boldsymbol{Y}_{\text{bus}}$.

Five DGs are located and sized by implementing the algorithm above for the standard 30-bus IEEE power system, as indicated in Table 5. The DGs can take discrete values between 0 and 5 MW/MVar for their P/Q with a 0.1 MW/MVar resolution. Additionally, the obtained results for the other optimisation variables are given in Table 6. The concept of the critical clearing time (CCT) for SGs and its well known equation are precisely discussed for the faults that occur at busbars in [53]. For further illustration, DG_i with a CCT of C_{DG} is assumed to be connected to busbar j. As a brief definition [53], if the duration of the fault occurrence at busbar j exceeds C_{DG}, then DG_i will never be stable after clearing the fault.

In the literature, DOCR coordination has been performed under this concept. However, transient stability analysis using the discussion provided in [53] is inaccurate for DOCR coordination. First, only faults on busbars are analysed, and faults on feeders are not developed for transient stability analysis, whereas DOCRs are responsible for faults on lines, not busbars. Consequently, the line percentage for which a DG remains stable cannot be obtained. Second, the power system configuration after clearing the fault is assumed to be the same as the network topology before fault occurrence. However, DOCRs can change the network topology by N feeders, which cannot be taken into account using the well known formulation developed by Grainger and Stevenson [53]. Finally, line resistances are assumed to be zero in [53]; however, this assumption may lead to inaccurate approximations. Although transient stability analysis using the introduced formulation has been frequently performed in the literature, this analysis is inaccurate for DOCR coordination.

In the following, transient stability analysis of DG_1 is performed for the situation, in which a fault occurs on line L_1, and relay R_1 is responsible for clearing the fault. In the first step, 21 faults are emulated on line L_1 with distances of 0, 5, 10, …, 100% of L_1 from R_1 and the voltages and currents of R_1 are measured for all cases. Afterwards, the operating times of R_1 for these 21 faults (T_0, T_5, T_{10}, …, T_{100}) are calculated based on the data provided in Table 6 and the measured voltages and currents.

Additionally, an electrical fault is simulated at 0% of L_1 (in front of R_1), and then, the R_1 circuit breaker is assumed to N L_1 following fault initiation with the previously calculated T_0 time difference. In the last step, the behaviour of the DG_1 rotor angle is observed in the next 1000 s. In this situation, if DG_1 becomes unstable, then R_1 fails to protect DG_1 from being unstable when a fault occurs in front of R_1. If DG_1 can reach a stable state (after fault clearance), then the next fault is simulated at 5% of L_1, and the DG_1 transient stability is checked similar to in the previous step.

The process above proceeds until R_1 fails to protect DG_1 from being unstable for a specific fault in front of R_1 at a specific distance. This obtained distance is provided for all DGs in Table 6 and 7. Additionally, the time difference between the fault appearance and circuit breaker operation in the last step is considered as the CCT of the DG. To be exact, the intersection between the CCT of the DG and DOCR reaction time signifies the specific fault distance (from corresponding DOCRs) which faults within this distance cannot disturb the transient stability of the DG.

Additionally, discrimination times for near- and far-end faults are shown in Fig. 8. The average discrimination times for near- and far-end faults are 0.3923 and 0.9022 s, respectively.

4.3 Complementary validations

In this section, DOCR coordination is performed considering the connection of the DGs with the optimised locations and sizes obtained in the previous section (Table 5). Besides the same network topology, the same optimisation method is implemented for coordination. Consequently, all coordination conditions are similar to those in the previous section. However, the non-standard relay curve proposed in [46] is taken for coordination, and these results are compared with those obtained using the non-standard relay curve proposed in (11). The DOCR coordination results obtained using the non-standard relay curve proposed in [46] are provided in Table 7.

Additionally, the discrimination times for near- and far-end faults are shown in Fig. 9. The average discrimination times for near- and far-end faults are 0.3217 and 1.5132 s, respectively. Having compared Fig. 8 with Fig. 9, it can be deduced that the obtained average discrimination time for far-end faults using the proposed method (0.9022 s) is remarkably less than the same quantity obtained using the relay curve proposed in [46].

An accurate comparison between Tables 6 and 7 reveals a total relay operating time reduction of 71.84% when using the proposed non-standard curve for coordination. Additionally, the summation of relay operating times for far-end faults exhibits a 5.24 s reduction.

The performance of the proposed method becomes more obvious compared with the other methods provided in the literature. In general, the minimum amount of the total relays operating time obtained in the previously reported research works was around 60 s for the 30-bus standard distribution network [7, 14, 15], while dual setting coordination scheme reduced this value to about 30 s [7, 15]. It is worth mentioning that applying RGP led to obtaining the total relays operating time in the range of dual setting approaches for the same power system using SI relays (see Table 1, [43]). Also, it was indicated in [43] that executing RGP using different types of relay curves (Table 1) can significantly decrease the total relays operating time (17.18 s) compared with the obtained result using dual setting methods (i.e. 30 s minimum). Subsequently, the total relays operating time significantly dropped to 4.187 s using the proposed approach which is in the range of 1/7th of dual setting methods and 1/15th of conventional overcurrent schemes. Comparing the results achieved for the 8-bus (Table 4) and the 30-bus (Table 4) power systems, it can be verified that as the number of the relay becomes larger, the difference between the results achieved using the proposed method becomes distinct from the results obtained implementing other approaches reported in the literature.

Table 6 Results for the 30-bus network using the proposed curve

RN	TSM	PSM	K	$t_{near\text{-}end}$	$t_{far\text{-}end}$	Transient stability
1	1.1837	1.5709	3.7683	0.0500	0.4571	DG1 100% of L_1
2	1.0735	1.2254	3.4357	0.0500	1.0006	DG2 100% of L_2
3	1.5892	1.5319	3.0990	0.1064	0.3500	DG1 100% of L_3
						DG2 100% of L_3
4	1.3744	1.4834	3.8006	0.0500	1.0330	DG2 100% of L_4
5	1.6141	1.4898	3.9256	0.0500	1.6362	
6	1.9174	1.3100	4.2018	0.0500	0.4369	
7	1.9091	1.6000	4.1758	0.0500	2.4827	
8	1.8409	1.3922	4.2762	0.0500	1.8418	
9	1.1701	1.4369	3.4092	0.0658	0.3500	
10	0.7821	1.5843	3.2083	0.0500	0.7430	
11	0.8259	1.4884	1.7710	0.2477	0.3669	DG3 100% of L_{11}
12	1.8451	1.2056	4.0001	0.0500	0.6070	
13	1.0295	1.4094	3.2710	0.0668	0.3500	DG3 100% of L_{13}
						DG4 100% of L_{13}
14	1.9947	1.3094	4.2753	0.0500	0.6934	
15	1.6689	1.5075	3.8384	0.0500	0.5452	DG4 100% of L_{15}
						DG5 100% of L_{15}
16	1.7678	1.6000	4.3687	0.0500	0.9953	DG5 100% of L_{16}
17	1.4282	1.2070	3.8704	0.0500	1.3068	
18	1.5499	1.2453	3.7797	0.0500	0.9272	
19	1.3510	1.4347	3.6399	0.0500	0.9180	DG5 100% of L_{19}
20	1.1188	1.3733	1.4853	0.5138	1.6561	DG1 100% of L_1
21	1.0162	1.2218	3.4145	0.0500	1.0929	DG2 100% of L_2
22	1.5533	1.5045	1.4821	0.5198	0.8138	DG1 100% of L_3
						DG2 100% of L_3
23	0.9695	1.4540	1.6920	0.3602	1.3140	DG2 100% of L_4
24	1.5701	1.5284	2.3181	0.3274	0.9387	
25	1.1023	1.5159	3.5450	0.0500	0.6320	
26	0.1200	1.2038	1.7425	0.0500	0.1855	
27	0.7644	1.4375	1.8422	0.3114	0.4105	
28	1.3607	1.2201	3.4655	0.0849	0.6292	
29	1.5509	1.2756	2.8982	0.1363	0.3849	DG3 100% of L_{11}
30	1.2774	1.4973	2.5111	0.1744	0.6114	
31	1.2925	1.2042	3.4974	0.0722	0.4363	DG3 100% of L_{13}
						DG4 100% of L_{13}
32	1.2828	1.5602	3.7058	0.0500	0.5774	
33	1.1934	1.4347	3.5008	0.0500	0.7242	DG4 100% of L_{15}
						DG5 100% of L_{15}
34	0.6570	1.2397	3.2655	0.0500	0.4657	DG5 100% of L_{16}
35	1.3212	1.3072	3.4828	0.0500	1.0571	DG5 100% of L_{20}
36	1.7340	1.2818	4.0048	0.0500	0.7467	
37	1.7812	1.5709	4.1566	0.0500	0.4247	DG5 100% of L_{19}
sum				4.1870	30.1422	

5 Conclusion

A novel relay curve robust to unforeseen inclination changes in voltage and current profiles measured by DOCRs in meshed networks was proposed. The proposed non-standard relay curve led to a satisfactory reduction in pair discrimination times considering the significant reduction in the total relay operating time. As a prominent optimiser, the DE algorithm in conjunction with RGP and Zoutendijk's method was applied to DOCR coordination optimisation problems. DOCR coordination was achieved for both the 8- and 30-bus IEEE standard power systems. The results obtained for these power systems were very satisfactory. To be exact, the total relay operating time obtained for the 30-bus IEEE standard system using the applied optimiser and non-standard relay curve was considerably less than half that for the 8-bus IEEE standard system using other optimisers and relay curves provided in the literature. Moreover, both near- and far-end faults were considered for coordination, and the obtained results considering the increase in the number of coordination constraints verified the robustness of the proposed method. Additionally, the proposed curve performance was more convenient as the power system became larger with more DOCRs and constraints, which confirmed the merits of the proposed relay curve once more.

6 Acknowledgments

The authors acknowledge financial support provided in part by the Faculty Development Competitive Research Grant (Project no. SOE2018018), the Nazarbayev University and in part by the Program-Targeted Funding of the Ministry of Education and

Table 7 Results for the 30-bus network using the curve proposed in [46]

RN	TSM	PSM	K	$t_{near\text{-}end}$	$t_{far\text{-}end}$	Transient stability
1	5.0000	1.5991	2.6788	0.6395	1.1160	DG1 100% of L_1
2	5.0000	1.6000	2.3031	0.7258	1.4985	DG2 100% of L_2
3	5.0000	1.5995	2.0605	1.0080	1.2567	DG1 100% of L_3
						DG2 100% of L_3
4	4.2241	1.2415	6.5085	0.0597	0.3505	DG2 100% of L_4
5	2.0727	1.4672	4.1730	0.0500	1.0651	
6	2.3764	1.4635	2.9195	0.2223	0.6073	
7	3.8086	1.4080	3.3168	0.2400	2.3306	
8	0.2293	1.5339	0.3651	0.3073	0.4809	
9	5.0000	1.5998	4.5526	0.0930	0.3698	
10	5.0000	1.6000	6.4267	0.0131	0.5660	
11	2.6983	1.3959	2.8498	0.2660	0.4159	DG3 100% of L_{11}
12	5.0000	1.6000	4.6797	0.0698	0.4219	
13	4.8837	1.4554	4.3283	0.1159	0.4111	DG3 100% of L_{13}
						DG4 100% of L_{13}
14	5.0000	1.6000	4.3388	0.1219	0.4137	
15	5.0000	1.3187	4.1393	0.1110	0.5170	DG4 100% of L_{15}
						DG5 100% of L_{15}
16	5.0000	1.6000	4.6069	0.1137	0.3754	DG5 100% of L_{16}
17	0.5838	1.3312	2.9291	0.0500	0.2490	
18	5.0000	1.6000	5.0062	0.0505	0.7064	
19	5.0000	1.5998	4.6106	0.0742	0.8710	DG5 100% of L_{19}
20	5.0000	1.6000	2.1037	1.2804	2.0264	DG1 100% of L_1
21	5.0000	1.5999	2.2600	0.8093	1.5569	DG2 100% of L_2
22	5.0000	1.6000	1.7957	1.3036	1.5804	DG1 100% of L_3
						DG2 100% of L_3
23	5.0000	1.5989	2.5689	0.7879	1.6867	DG2 100% of L_4
24	5.0000	1.6000	3.5263	0.3214	1.0879	
25	5.0000	1.5991	3.6989	0.1967	0.6899	
26	2.9045	1.4180	1.6323	1.3192	2.4733	
27	3.5982	1.2686	2.3321	0.9166	1.0258	
28	5.0000	1.5996	3.0435	0.4915	1.0258	
29	5.0000	1.5994	2.8334	0.5026	0.7915	DG3 100% of L_{11}
30	5.0000	1.5986	2.3853	0.8223	1.2166	
31	5.0000	1.6000	3.4517	0.2978	0.8026	DG3 100% of L_{13}
						DG4 100% of L_{13}
32	5.0000	1.5999	2.9763	0.4345	1.4167	
33	4.9986	1.5992	4.5285	0.0754	0.5978	DG4 100% of L_{15}
						DG5 100% of L_{15}
34	5.0000	1.6000	3.9268	0.2032	0.7346	DG5 100% of L_{16}
35	1.6305	1.2974	3.7021	0.0500	0.3885	DG5 100% of L_{20}
36	5.0000	1.5997	2.6795	0.5710	1.7539	
37	5.0000	1.5989	3.8277	0.2077	0.5032	DG5 100% of L_{19}
sum				14.8731	35.3813	

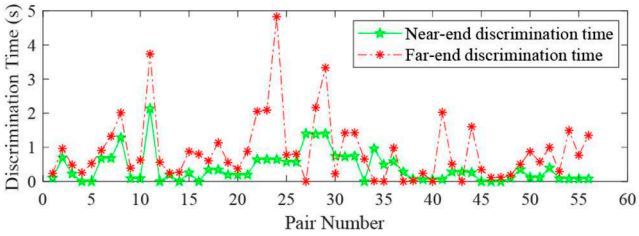

Fig. 8 *Near/far-end discrimination times using the proposed relay curve*

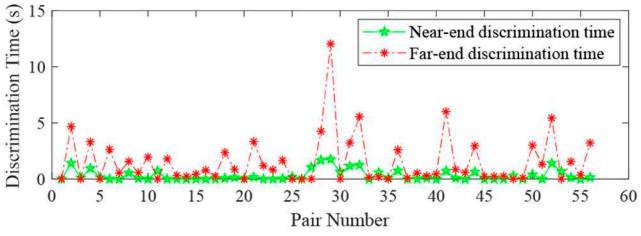

Fig. 9 *Near/far-end discrimination times using the curve proposed in [46]*

Science of the Republic of Kazakhstan through the Innovative Materials and Systems for Energy Conversion and Storage for 2018–2020 under Grant no. BR05236524.

7 References

[1] Hamidi, M.E., Mohammadi Chabanloo, R.: 'Optimal allocation of distributed generation with optimal sizing of fault current limiter to reduce the impact on

distribution networks using NSGA-II', *IEEE Syst. J.*, 2019, **13**, (2), pp. 1714–1724
[2] Yazdanpanahi, H., Wei Li, Y., Xu, W.: 'A new control strategy to mitigate the impact of inverter-based DGs on protection system', *IEEE Trans. Smart Grid.*, 2012, **3**, (3), pp. 1427–1436
[3] Shih, M.Y., Conde, A., Leonowicz, Z., *et al.*: 'An adaptive overcurrent coordination scheme to improve relay sensitivity and overcome drawbacks due to distributed generation in smart grids', *IEEE Trans. Ind. Appl.*, 2017, **53**, (6), pp. 5217–5228
[4] Nabab Alam, M.: 'Adaptive protection coordination scheme using numerical directional overcurrent relays', *IEEE Trans. Ind. Inf.*, 2019, **15**, (1), pp. 64–73
[5] Brahma, S.M., Girgis, A.A.: 'Development of adaptive protection scheme for distribution systems with high penetration of distributed generation', *IEEE Trans. Power Deliv.*, 2004, **19**, (1), pp. 56–63
[6] Wan, H., Li, K.K., Wong, K.P.: 'An adaptive multiagent approach to protection relay coordination with distributed generators in industrial power distribution system', *IEEE Trans. Ind. Appl.*, 2010, **46**, (5), pp. 2118–2124
[7] Zeineldin, H.H., Sharaf, H.M., Ibrahim, D.K., *et al.*: 'Optimal protection coordination for meshed distribution systems with DG using dual setting directional overcurrent relays', *IEEE Trans. Smart Grid*, 2015, **6**, (1), pp. 115–123
[8] Solati Alkaran, D., Vatani, M.R., Sanjari, M.J., *et al.*: 'Overcurrent relays coordination in interconnected networks using accurate analytical method and based on determination of fault critical point', *IEEE Trans. Power Deliv.*, 2015, **30**, (2), pp. 870–877
[9] Solati Alkaran, D., Vatani, M.R., Sanjari, M.J.: 'Optimal overcurrent relay coordination in interconnected networks by using fuzzy-based GA method', *IEEE Trans. Smart Grid*, 2018, **9**, (4), pp. 3091–3101
[10] Wheeler, K.A., Elsamahy, M., Farid, S.H.: 'A novel reclosing scheme for mitigation of distributed generation effects on overcurrent protection', *IEEE Trans. Power Deliv.*, 2018, **33**, (2), pp. 981–991
[11] Naiem, A.F., Hegazy, Y., Abdolaziz, A.Y., *et al.*: 'A classification technique for recloser–fuse coordination in distribution systems with distributed generation', *IEEE Trans. Power Deliv.*, 2012, **27**, (1), pp. 176–185
[12] Hussain, B., Sharkh, S.M., Hussain, S., *et al.*: 'An adaptive relaying scheme for fuse saving in distribution networks with distributed generation', *IEEE Trans. Power Deliv.*, 2013, **28**, (2), pp. 669–677
[13] Amraee, T.: 'Coordination of directional overcurrent relays using seeker algorithm', *IEEE Trans. Power Deliv.*, 2012, **27**, (3), pp. 1415–1422
[14] Papaspiliotopoulos, V.A., Korres, G.N., Maratos, N.G.: 'A novel quadratically constrained quadratic programming method for optimal coordination of directional overcurrent relays', *IEEE Trans. Power Deliv.*, 2017, **32**, (1), pp. 3–10
[15] Sharaf, H.M., Zeineldin, H.H., Sadaany, E.E.: 'Protection coordination for microgrids with grid-connected and islanded capabilities using communication assisted dual setting directional overcurrent relays', *IEEE Trans. Smart Grid*, 2018, **9**, (1), pp. 143–151
[16] Nikolaidis, V.C., Papanikolaou, E., Safigianni, A.S.: 'A communication-assisted overcurrent protection scheme for radial distribution systems with distributed generation', *IEEE Trans. Smart Grid*, 2016, **7**, (1), pp. 114–123
[17] Coffele, F., Booth, C., Dysko, A.: 'An adaptive overcurrent protection scheme for distribution networks', *IEEE Trans. Power Deliv.*, 2015, **30**, (2), pp. 561–568
[18] Mahat, P., Chen, Z., Jensen, B.B., *et al.*: 'A simple adaptive overcurrent protection of distribution systems with distributed generation', *IEEE Trans. Smart Grid*, 2011, **2**, (3), pp. 428–437
[19] Laaksonen, H., Ishchenko, D., Oudalov, A.: 'Adaptive protection and microgrid control design for Hailuoto island', *IEEE Trans. Smart Grid*, 2014, **5**, (3), pp. 1486–1493
[20] Tjahjono, A., Anggriawan, D.O., Faizin, A.K.: 'Adaptive modified firefly algorithm for optimal coordination of overcurrent relays', *IET Gener. Transm. Distrib.*, 2017, **11**, (10), pp. 2575–2585
[21] Shih, M.Y., Salazar, C.A.C., Enriquez, A.C.: 'Adaptive directional relay overcurrent coordination using ant colony optimization', *IET Gener. Transm. Distrib.*, 2015, **9**, (14), pp. 2040–2049
[22] Mohammadi Chabanloo, R., Safari, M., Gholizadeh Roshanagh, R.: 'Reducing the scenarios of network topology changes for adaptive coordination of overcurrent relays using hybrid GA–LP', *IET Gener. Transm. Distrib.*, 2018, **12**, (21), pp. 5879–5890
[23] El-khattam, W., Sidhu, T.S.: 'Resolving the impact of distributed renewable generation on directional overcurrent relay coordination: a case study', *IET Renew. Power Gener.*, 2009, **3**, (4), pp. 415–425
[24] Huchel, Ł., Zeineldin, H.H.: 'Planning the coordination of directional overcurrent relays for distribution systems considering DG', *IEEE Trans. Smart Grid*, 2016, **7**, (3), pp. 1642–1649
[25] Sharma, A., Kiran, D., Panigrahi Bijaya, K.: 'Planning the coordination of overcurrent relays for distribution systems considering network reconfiguration and load restoration', *IET Gener. Transm. Distrib.*, 2018, **12**, (7), pp. 1672–1679
[26] Dehghanpour, E., Karegar, H.K., Kheirollahi, R., *et al.*: 'Optimal coordination of directional overcurrent relays in microgrids by using cuckoo-linear optimization algorithm and fault current limiter', *IEEE Trans. Smart Grid*, 2018, **9**, (2), pp. 1365–1375
[27] Najy, W.K.A., Zeineldin, H.H., Woon, W.L.: 'Optimal protection coordination for microgrids with grid-connected and islanded capability', *IEEE Trans. Ind. Electron.*, 2013, **60**, (4), pp. 1668–1677
[28] Chaitusaney, S., Yokoyama, A.: 'Prevention of reliability degradation from recloser–fuse miscoordination due to distributed generation', *IEEE Trans. Power Deliv.*, 2008, **23**, (4), pp. 2545–2554
[29] Salem, M.M., Elkalashi, L.I., Atia, Y., *et al.*: 'Modified inverter control of distributed generation for enhanced relaying coordination in distribution networks', *IEEE Trans. Power Deliv.*, 2017, **32**, (1), pp. 78–87
[30] Meyer, R., Zelotnic, A., Mertens, A.: 'Fault ride through control of medium-voltage converters with LCL filter in distributed generation systems', *IEEE Trans. Ind. Appl.*, 2014, **50**, (5), pp. 3448–3456
[31] Piya, P., Ebrahimi, M., Karimi-Ghartemani, M., *et al.*: 'Fault ride-through capability of voltage-controlled inverters', *IEEE Trans. Ind. Electron.*, 2018, **65**, (10), pp. 7933–7943
[32] Zhan, H., Wang, C., Wang, Y., *et al.*: 'Relay protection coordination integrated optimal placement and sizing of distributed generation sources in distribution networks', *IEEE Trans. Smart Grid*, 2016, **7**, (1), pp. 55–65
[33] Ojaghi, M., Mohammadi, V.: 'Use of clustering to reduce the number of different setting groups for adaptive coordination of overcurrent relays', *IEEE Trans. Power Deliv.*, 2018, **33**, (3), pp. 1204–1212
[34] Xyngi, I., Popov, M.: 'An intelligent algorithm for the protection of smart power systems', *IEEE Trans. Smart Grid.*, 2013, **4**, (3), pp. 1541–1548
[35] Srivastava, A., Tripathy, J.M., Krishan, R., *et al.*: 'Optimal coordination of overcurrent relays using gravitational search algorithm with DG penetration', *IEEE Trans. Ind. Appl.*, 2018, **54**, (2), pp. 1155–1165
[36] Costa, M.H., Saldanha, R.R., Ravetti, M.G., *et al.*: 'Robust coordination of directional overcurrent relays using a metaheuristic algorithm', *IET Gener. Transm. Distrib.*, 2017, **11**, (2), pp. 464–474
[37] Saha, D., Datta, A., Das, P.: 'Optimal coordination of directional overcurrent relays in power systems using symbiotic organism search optimization technique', *IET Gener. Transm. Distrib.*, 2016, **10**, (11), pp. 2681–2688
[38] Baghaee, H.R., Mirsalim, M., Gharehpetian, G.B., *et al.*: 'MOPSO/FDMT-based Pareto-optimal solution for coordination of overcurrent relays in interconnected networks and multi-DER microgrids', *IET Gener. Transm. Distrib.*, 2018, **12**, (12), pp. 2871–2886
[39] Purwar, E., Vishwakarma, D.N., Singh, S.P.: 'A novel constraints reduction based optimal relay coordination method considering variable operational status of distribution system with DGs', *IEEE Trans. Smart Grid*, 2019, **10**, (1), pp. 889–898
[40] Saberi Noghabi, A., Sadeh, J., Rajabi Mashhadi, H.: 'Considering different network topologies in optimal overcurrent relay coordination using a hybrid GA', *IEEE Trans. Power Deliv.*, 2009, **24**, (4), pp. 1857–1863
[41] Bedekar, P.P., Bhide, S.R.: 'Optimum coordination of directional overcurrent relays using the hybrid GA-NLP approach', *IEEE Trans. Power Deliv.*, 2011, **26**, (1), pp. 109–119
[42] Radosavljević, J., Jevtić, M.: 'Hybrid GSA-SQP algorithm for optimal coordination of directional overcurrent relays', *IET Gener. Transm. Distrib.*, 2016, **10**, (8), pp. 1928–1937
[43] Darabi, A., Bagheri, M., Gharehpetian, G.B.: 'Highly accurate directional overcurrent coordination via combination of Rosen's gradient projection-complex method with GA–PSO algorithm', *IEEE Syst. J.*, 2019, Print ISSN:1932-8184. Electronic ISSN: 1937-9234 Early access: https://ieeexplore.ieee.org/document/8680630, pp. 1–12
[44] Rao, S.S.: Engineering optimization: theory and practice, Fourth Edition, 2009
[45] Jamali, S., Borhani-Bahabadi, H.: 'Non-communication protection method for meshed and radial distribution networks with synchronous-based DG', *Electr. Power Energy Syst.*, 2017, **93**, pp. 468–478
[46] Saleh, K.A., Zeineldin, H.H., Al-Hiani, A., *et al.*: 'Optimal coordination of directional overcurrent relays using a new time–current–voltage characteristic', *IEEE Trans. Power Deliv.*, 2015, **30**, (2), pp. 537–544
[47] Kılıçkıran, H.C., Akdemir, H., Sengor, I., *et al.*: 'A non-standard characteristic based protection scheme for distribution networks', *Energies*, 2018, **11**, (5), p. 1241
[48] Jamali, S., Borhani-Bahabadi, H.: 'Self-adaptive relaying scheme of reclosers for fuse saving in distribution networks with DG', *Int. J. Power Energy Res.*, 2017, **1**, (1), pp. 8–19
[49] Kılıçkıran, H.C., Sengor, I., Akdemir, H., *et al.*: 'Power system protection with digital overcurrent relays: a review of non-standard characteristics', *Electr. Power Syst. Res.*, 2018, **164**, pp. 89–102
[50] Gers, J., Holmes, E.: 'Protection of electricity distribution networks', '*ser. IET power and energy series*' (Institution of Engineering and Technology, 2011, 3rd edn.), p. 368, ISBN-13: 978-1-84919-223-1
[51] Rajput, V.N., Pandya, K.: 'On 8-bus test system for solving challenges in relay coordination'. IEEE International Conf. Power Systems Conf., Delhi, India, 4–6 March 2016
[52] Available at http://www.ee.washington.edu/research/pstca/
[53] Grainger, J.J., Stevenson, W.D.: 'Power system analysis', 1994